Global and Planetary Change 65 (2009) 1–11

Contents lists available at ScienceDirect

Global and Planetary Change

journal homepage: www.elsevier.com/locate/gloplacha

Tree ring density-based summer temperature reconstruction for the central Hengduan Mountains in southern China

Ze-Xin Fan [a,b], Achim Bräuning [b,*], Bao Yang [c], Kun-Fang Cao [a]

[a] Xishuangbanna Tropical Botanical Garden, the Chinese Academy of Sciences, 88 Xuefu Road, Kunming 650223, China
[b] Institute of Geography, University of Erlangen-Nürnberg, Kochstrasse 4/4, D-91054 Erlangen, Germany
[c] Cold and Arid Regions Environmental and Engineering Research Institute, the Chinese Academy of Sciences, 260 Donggang West Road, Lanzhou 730000, China

ARTICLE INFO

Article history:
Received 11 June 2008
Accepted 2 October 2008
Available online 17 October 2008

Keywords:
dendroclimatology
Hengduan Mountains
maximum latewood density
ring width
temperature

ABSTRACT

Variations in ring width and wood density of *Picea brachytyla* were used to develop high-resolution climate proxy data to extend the existing climate record in the central Hengduan Mountains, north-western Yunnan Province, China. Growth–climate response analyses showed that the total ring width (TRW) and maximum latewood density (MXD) in the sub-alpine zone are mainly influenced by summer temperature variability. Based on a MXD regional chronology derived from two high elevation sites, we developed a warm season (April–September) temperature reconstruction for the period A.D. 1750–2006. The climate/tree-growth model accounts for 41% of the instrumental temperature variance during the period 1958–2004. Warm summers occurred during 1750s, 1820–50s, 1880–1890s, 1930–1950s and 1990–present; while the periods of 1790–1810s, 1860–1870s, 1900–1920s, and 1960–1985 were relatively cold. Spatial climate correlation analyses with gridded land surface data revealed that our warm season temperature reconstruction contains a strong regional temperature signal for the Hengduan Mountain ranges. Our reconstruction successfully captured recent abrupt climatic changes and agreed in general with other tree ring-based temperature reconstructions from nearby regions on a decadal timescale. In addition, reconstructed summer temperature variations were consistent with recorded glacier fluctuations in the surrounding high mountains.

1. Introduction

The Tibetan Plateau, with an average elevation above 4000 m a.s.l. and an extension of more than 2 million km^2, plays a key role in driving the Asian summer monsoon circulation (Webster et al., 1998). Understanding of spatial and temporal climate variations over the Tibetan Plateau is thus vital to improve our knowledge of Asian monsoon dynamics. However, meteorological records over the Tibetan Plateau are short and sparse in spatial distribution, which limits our ability to examine current climate regimes in a long-term perspective. High resolution proxy data like tree rings are needed to shed more light on the climate variability of the Tibetan Plateau.

Tree-ring series, especially maximum latewood density from cold-moist sites have great potential for the reconstruction of summer temperatures on regional to hemispheric scales, reflecting inter-annual to multi-centennial scale variability (e.g. Schweingruber and Briffa, 1996; Briffa et al., 2001; Frank and Esper, 2005; Büntgen et al., 2006, 2008). Many of the density-related studies, however, were carried out in the boreal and temperate climate zones of North America (Wang et al., 2001; Davi et al., 2003; D'Arrigo et al., 2004; Luckman and Wilson, 2005), Siberia (Briffa et al., 2001; Kirdyanov et al., 2008) and Europe (Briffa et al., 1988, 2004; Büntgen et al., 2008). Concerning the high mountain areas of China, century- to millennial-scale temperature fluctuations were reconstructed for north-eastern Tibet (e.g. Kang et al., 1997; Liu et al., 2005; Gou et al., 2007) and for the southern parts of the Tibetan Plateau (Wu et al., 1989; Bräuning, 1994; Bräuning and Mantwill, 2004). However, the density of the available tree-ring data is still sparse, and most studies were based on total ring width (TRW). A combination of the wood parameters TRW and maximum latewood density (MXD) may reflect different temperature seasonality (Bräuning, 2001; Bräuning and Grießinger, 2006).

Despite of their widespread forest cover, only few dendroclimatological studies have been conducted in the north–south oriented Hengduan Mountain ranges, which form the southern rim of the Tibetan Plateau and are strongly exposed to the South Asian summer monsoon (Wu et al., 1988; Shao and Fan, 1999; Bräuning and Mantwill, 2004). Using four ring-width chronologies, Shao and Fan (1999) reconstructed winter season minimum temperature for the eastern part of the Hengduan Mountains on the West Sichuan Plateau. Wu et al. (1988) reported an annual temperature reconstruction for the Hengduan Mountains, but no information about the strength of the tree growth–climate signal or the reliability of the reconstruction was provided. In addition, their data lack information about climatic

* Corresponding author. Tel.: +49 9131 8529372; fax: +49 9131 8522013.
E-mail address: abraeuning@geographie.uni-erlangen.de (A. Bräuning).

0921-8181/$ – see front matter © 2008 Elsevier B.V. All rights reserved.
doi:10.1016/j.gloplacha.2008.10.001

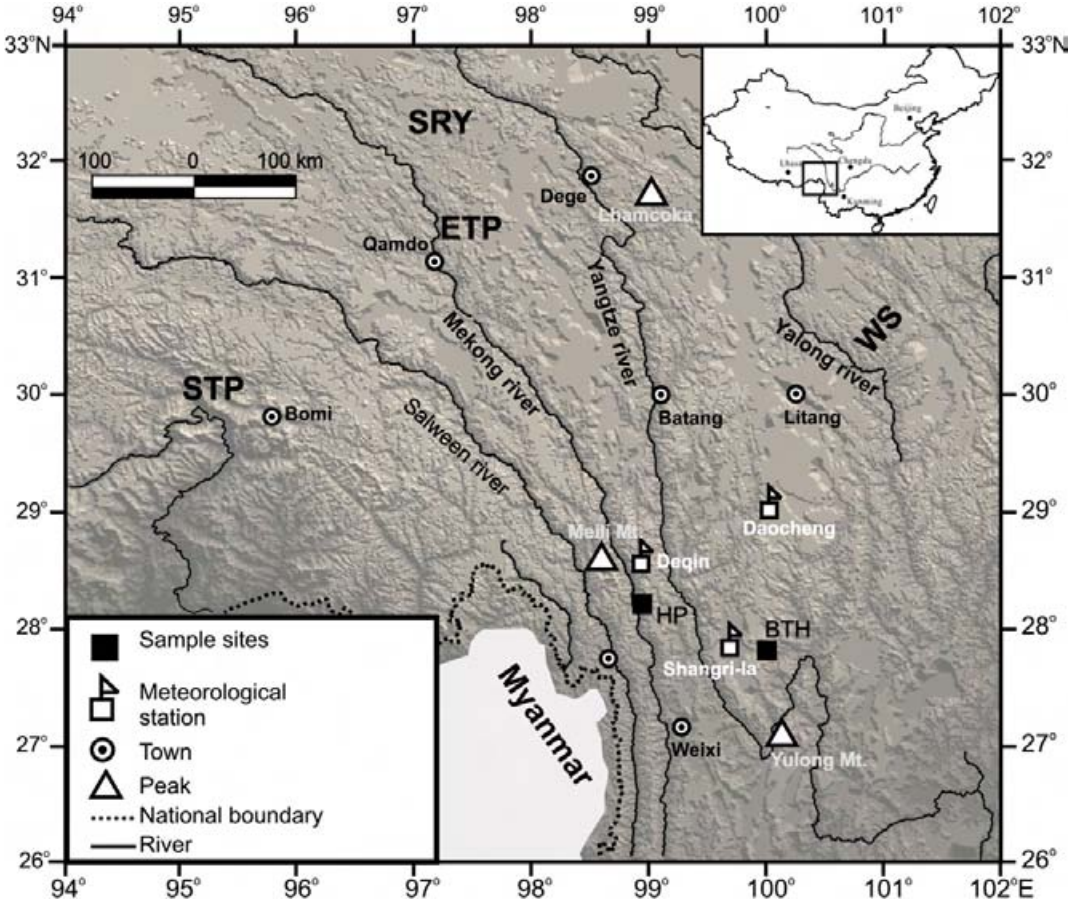

Fig. 1. Map showing the locations of tree-ring sample sites and meteorological stations. Bold letters show the locations of the tree-ring based temperature reconstructions from the south (STP) and eastern (ETP) Tibetan Plateau (Bräuning and Mantwill, 2004), the upper source region of Yangtze River (SRY; Liang et al., 2008) and west Sichuan Plateau (WS; Shao and Fan, 1999).

changes after A.D. 1981. Based on a network of 22 MXD chronologies of high elevation conifer sites, late summer temperature over the past 400 years was reconstructed for the southeastern Tibetan Plateau directly to the north of our study region (Bräuning and Mantwill, 2004).

In this paper, we present new tree-ring chronologies of TRW and MXD from *Picea brachytyla* located in the central Hengduan Mountain ranges. We analyze the relationships between tree-ring parameters and their climatic forcing. Based on MXD data, we reconstruct warm season (April–September) temperatures over the A.D. 1750–2006

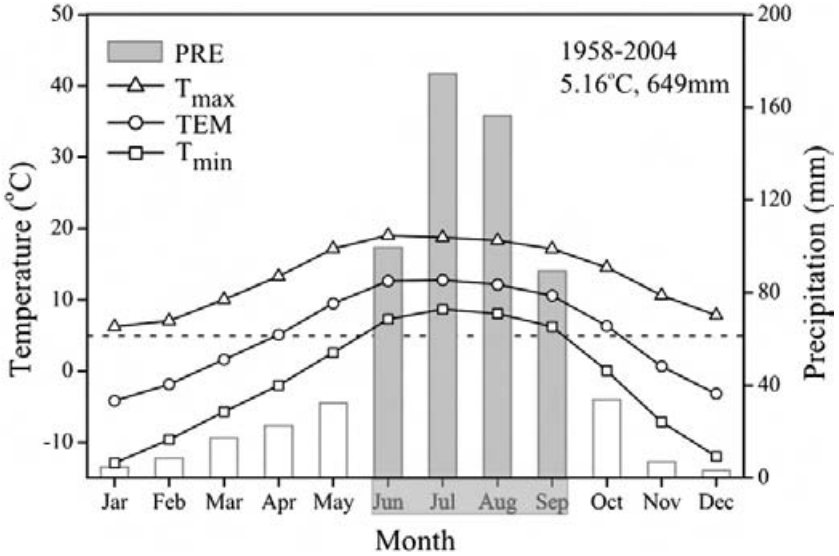

Fig. 2. Monthly total precipitation (bars) and maximum (line with triangles), mean (line with circles) and minimum (line with squares) temperatures for the central Hengduan Mountains, derived from meteorological records of Shangri-la and Daocheng. The dashed line indicates a 5 °C temperature threshold. Gray bars highlight the summer season.

Table 1
Site information and tree-ring chronologies statistics. HP, Hongpo at Baima Snow Mountain; BTH, Bitahai Nature Reserve; RC, regional chronology; TRW, total ring width; MXD, maximum latewood density; Lat., latitude; Lon., longitude; Elev., elevation; C/T, cores/trees; MSL, mean segment length; SD, standard deviation; MS, mean sensitivity; AC1, first-order autocorrelation; Rbar, mean inter-series correlation; EPS>0.85, year/no. of cores when expressed population signal exceeds the 0.85 threshold

Site	Date type	Location (Lat./Lon.)	Elev. (m)	C/T	Time span (A.D.)	MSL	SD[a]	MS[a]	AC1[a]	Rbar[b]	EPS>0.85[b]
HP	TRW	28.25/98.91	3500	80/51	1688–2005	186	0.28	0.20	0.70	0.59	1780/21
	MXD			31/29	1724–2005	179	0.14	0.11	0.51	0.41	1820/15
BTH	TRW	27.82/99.99	3580	50/40	1623–2007	234	0.22	0.15	0.65	0.48	1690/17
	MXD			31/29	1623–2006	235	0.15	0.11	0. 59	0.46	1750/17
RC	TRW			130/91	1623–2007	204	0.25	0.18	0.68	0.46	1690/18
	MXD			62/58	1623–2006	207	0.15	0.11	0.55	0.39	1750/20

[a] Calculated for ARSTAN standard chronologies.
[b] Calculated for ARSTAN residual chronologies for 30-year intervals with 15-year overlaps.

period of reliable internal signal strength. This new record is then compared with existing findings from nearby regions.

2. Geographical settings

The study area is located in the central Hengduan Mountain ranges, north-western Yunnan Province, China (Fig. 1). The region is well known for its high levels of biodiversity owing to the steep topographic gradients resulting from the Mekong, Yangtze, Salween and Irrawaddy rivers which cut deep, north–south oriented gorges in the mountainous landscape during their descent from the Tibetan Plateau. The region's climate is temperate and is characterized by a precipitation maximum during the summer months. Summer precipitation originates from monsoonal air masses flowing over the Bay of Bengal, whereas winters are generally dry (Xu et al., 2003). The deeply incised gorges of the parallel rivers form pathways for the monsoonal air masses, resulting in a steep moisture gradient from south–east to north–west in southern Tibet (Chang, 1981). According to the regional average of instrumental stations in Shangri-la and Daocheng, the mean annual temperature is 5.16 °C, with a mean temperature of 12.7 °C in July and −4.2 °C in January. Mean annual total precipitation is 649 mm. The precipitation in the summer season (June to September) accounts for 80% of the annual total precipitation (Fig. 2).

3. Materials and methods

3.1. Sampling

P. brachytyla var. *complanata* is a shade-tolerant species, dominating the sub-alpine altitudinal vegetation zone between 2800 and 3900 m in the mountain area of north-western Yunnan Province. Two sites of *P. brachytyla* were chosen in forests near the upper timberline. The Hongpo (HP) site (28.25 °N, 98.91 °E, 3500 m a.s.l.) was located on the west slope of the Baima Snow Mountains. The Bitahai (BTH) site (27.82 °N, 99.99 °E, 3580 m a.s.l.), ~120 km south-east of the HP site, was located in the Bitahai Nature Reserve (Fig. 1). Totally, 130 increment cores from 91 trees were extracted with an increment borer at breast height.

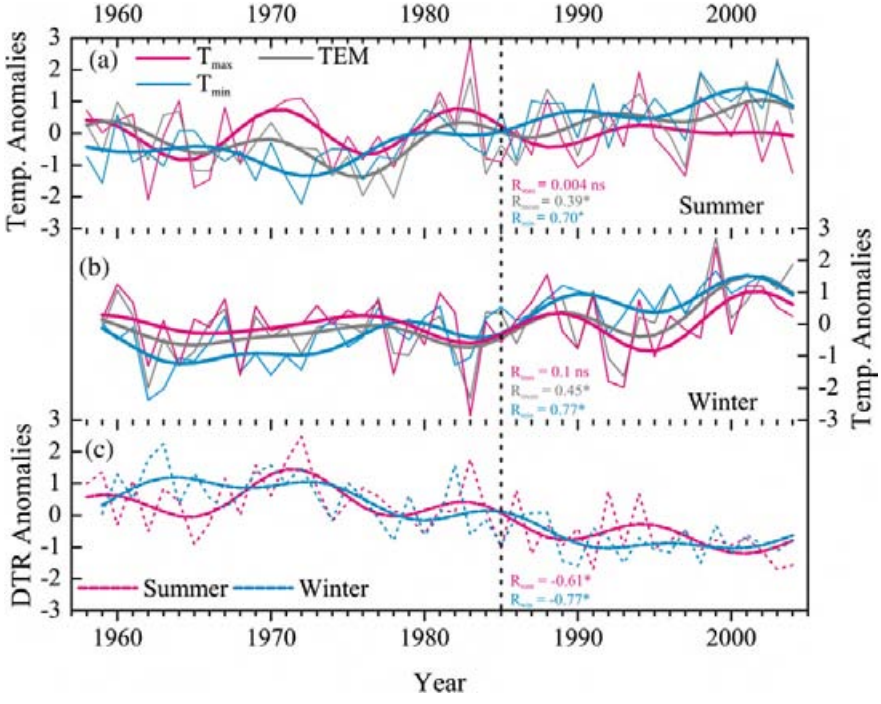

Fig. 3. Temporal changes of regional monthly maximum (T_{max}), mean (TEM), minimum (T_{min}) temperature in the summer (a, June–September) and winter (b, prior November–February) seasons; (c) temporal changes of regional diurnal temperature range (DTR). Values are expressed as anomalies (reference period=1959–2004) and bold lines were smoothed using a 10-year low-pass filter.

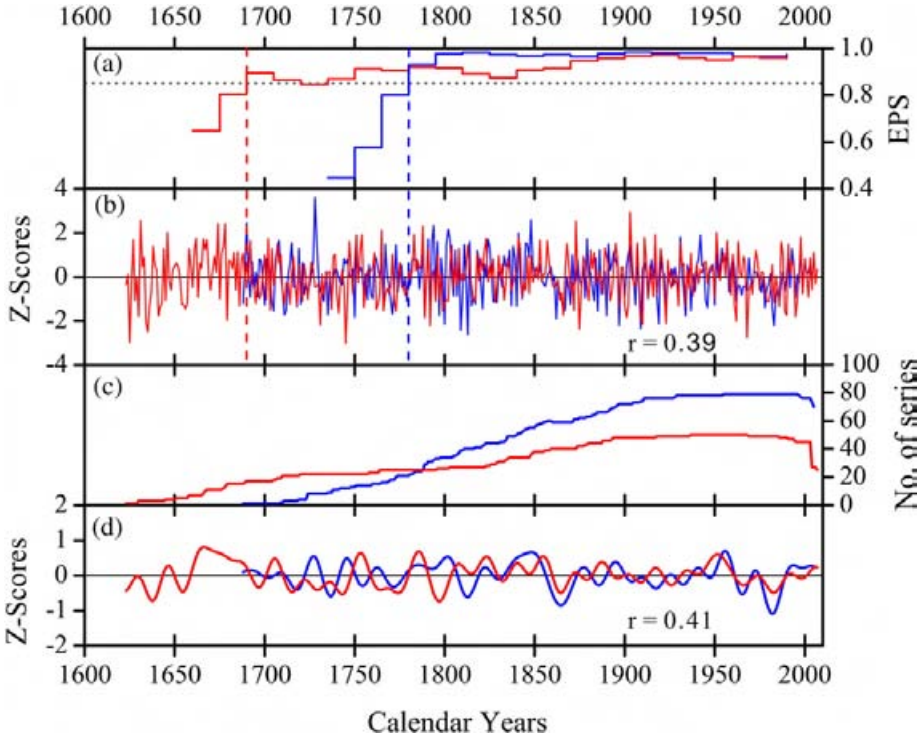

Fig. 4. Comparison between the HP (blue) and BTH (red) ring-width residual chronologies. (a) Expressed population signal (EPS) statistic (calculated over 30 years lagged by 15 years); (b) the two residual chronologies adjusted to the same mean and variance over the common period 1688–2005; (c) the sample depth through time; (d) the 15-year low-pass filtered components. The correlation coefficients were calculated for 1780–2005 when EPS exceeds the threshold of 0.85 for both chronologies.

3.2. Chronology development

Chronologies were developed for the two parameters TRW and MXD. The surface of cores was prepared with razor blades and the surface contrast was enhanced with chalk. Ring widths were registered with a LINTAB II measuring system with a resolution of 0.01 mm, and all cores were cross-dated visually and using statistical tests (sign-test and *t*-test) (Stokes and Smiley, 1996; Rinn, 1996). 62

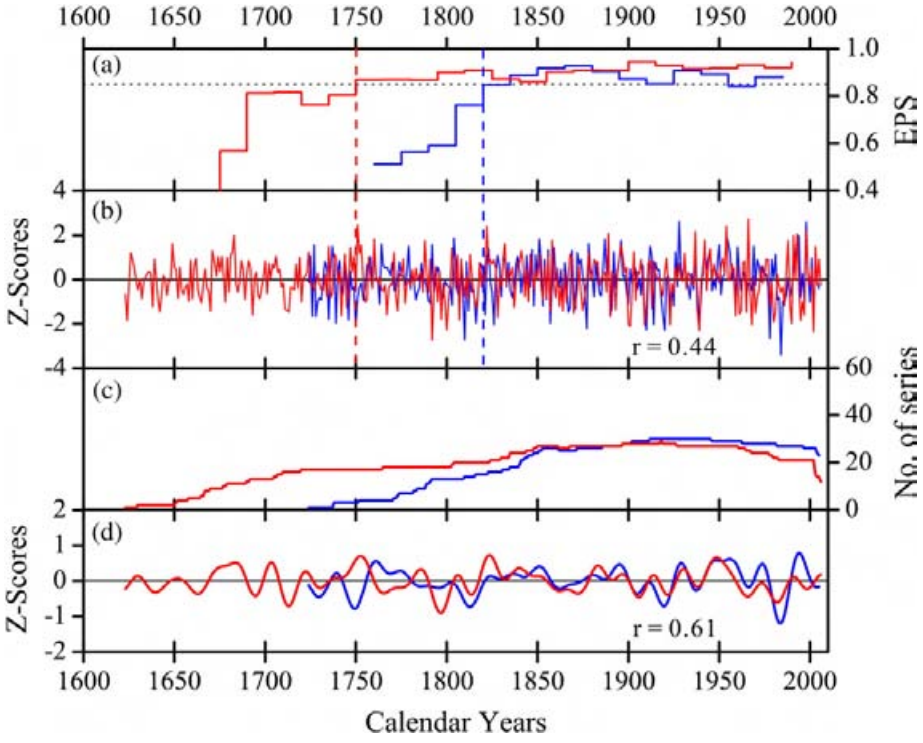

Fig. 5. Comparison between the HP (blue) and BTH (red) maximum latewood density residual chronologies. (a) Expressed population signal (EPS) statistic (calculated over 30 years lagged by 15 years); (b) the two residual chronologies adjusted to the same mean and variance over the common period 1724–2005; (c) the sample depths through time; (d) their 15-year low-pass filtered components. The correlation coefficients were calculated for 1820–2005 when EPS exceeds the threshold of 0.85 for both chronologies.

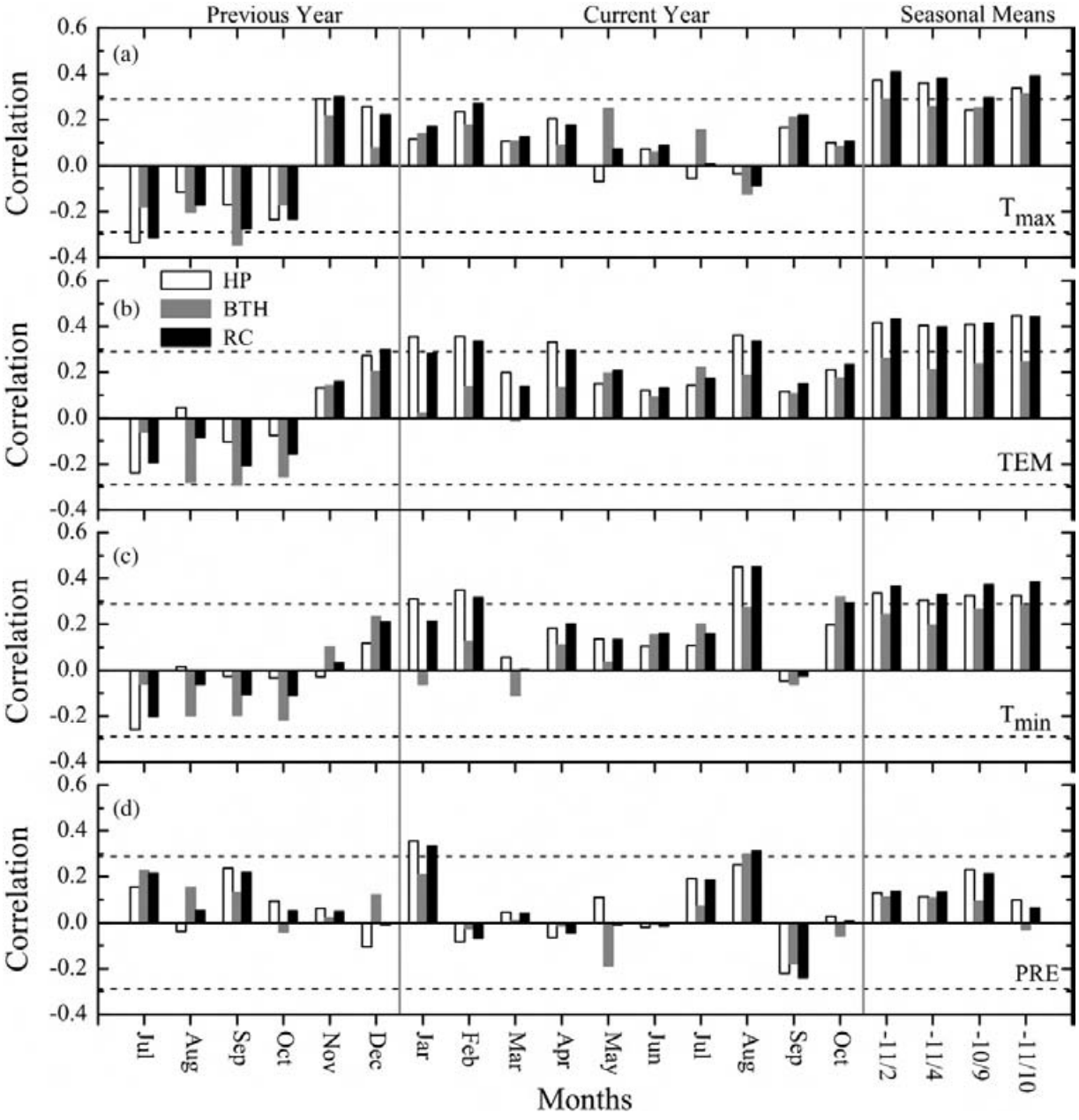

Fig. 6. Climate response of ring width (TRW) for the sites HP (white), BTH (grey) and their regional chronology (RC, black) using (a) maximum temperatures (T_{max}), (b) mean temperatures (TEM), (c) minimum temperatures (T_{min}), and (d) precipitation sums (PRE). Correlations were calculated from previous year July to current year October over 1958–2004 common periods. Horizontal dashed lines denote the 95% significance levels. Numbers on x-axis refer to seasonal means of prior November–February (−11/2), prior November–April (−11/4), prior October–September (−10/9), and prior November–October (−11/10), respectively.

cores (58 trees) with high wood quality (i.e. without wood decomposition by fungal attack) were further processed for density measurement using the Lignostation densitometry system (Rinntech, Germany; Schinker et al., 2003). Relative density variations were measured along smoothed wood surfaces using a high-frequency dielectric scanner with a spatial resolution of 10 μm. For each ring, six parallel paths were scanned with a distance-in-between ≥0.1 mm, and a mean value was calculated from the six density profiles. Although earlywood width, latewood width, minimum and maximum density were also determined for each year, only TRW and MXD data were used in this study as they have consistently proved to be the best tree-ring parameters for the reconstruction of past temperatures (Briffa et al., 2004; Bräuning and Mantwill, 2004; Luckman and Wilson, 2005).

In order to remove biological trends associated with tree-age (Fritts, 1976) while preserving variations that are likely related to climate, the tree ring series were standardized to dimensionless indices using the program ARSTAN (Cook, 1985). Prior to standardization, the variance of each series was stabilized using a data-adaptive power transformation based on the individual mean and standard deviation (Cook and Peters, 1997). The TRW measurements were standardized by first adjusting a negative exponential or a linear regression function to the raw data, and then the resulting sequences were detrended with a cubic smoothing spline with a 50% frequency-response cut-off equal to 2/3 of the series length. The only age-related trend in most MXD series is a linear decrease of maximum density with age. Therefore, MXD series were detrended using negative or zero slope linear regression functions. This process removes or reduces the influence of disturbance and changes in tree growth with age, while preserving inter-annual to multi-decadal scale variability in the tree-ring series.

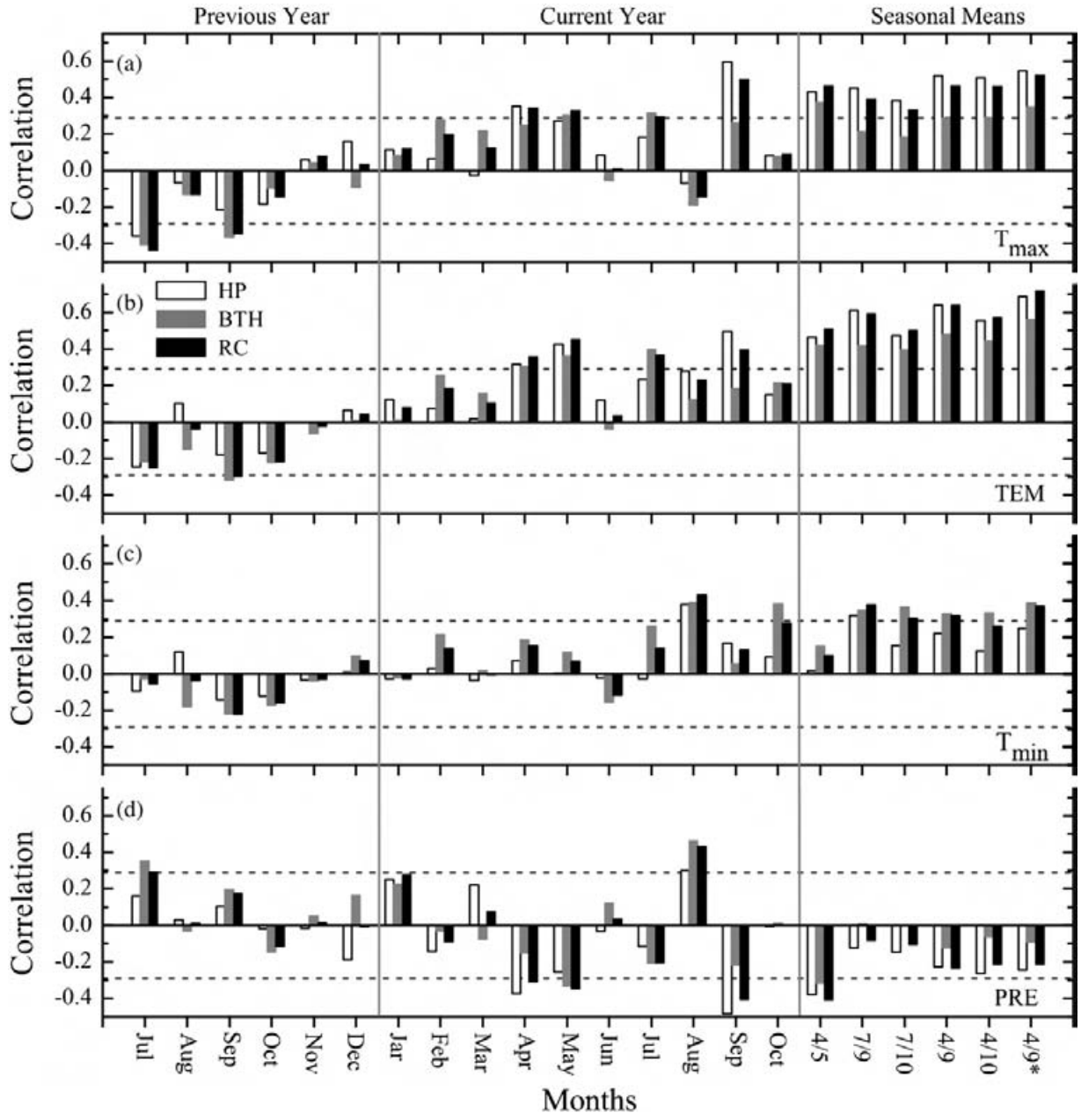

Fig. 7. Climate response of maximum latewood density (MXD) for the sites HP (white), BTH (grey) and their regional chronology (RC, black) using (a) maximum temperatures (T_{max}), (b) mean temperatures (TEM), (c) minimum temperatures (T_{min}) and (d) precipitation sums (PRE). Correlations were calculated from previous year July to current year October over 1958–2004 common periods. Horizontal dashed lines denote the 95% significance levels. Numbers on x-axis refer to seasonal means of April–May (4/5), July–September (7/9), April–September (4/9), April–October (4/10), April–September but excluding June (4/9*), respectively.

Autoregressive modelling was used to remove persistence from tree-ring series, producing pre-whitened 'residual' indices (Cook, 1985). All detrended series were averaged to chronologies by computing the biweight robust mean in order to reduce the influence of outliers (Cook and Kairiukstis, 1990). In order to reduce the influence of decreasing sample size in the older parts of the chronologies, the chronology variance was stabilized using the method described by Osborn et al. (1997). The inter-series correlation (Rbar) and expressed population signal (EPS) were employed to evaluate the most reliable periods of internal signal strength (Wigley et al., 1984). Both Rbar and EPS were calculated for pre-whitened residuals for 30-year moving windows with 15-year overlaps, and a level of 0.85 in EPS was considered to indicate a satisfactory quality of a chronology (Wigley et al., 1984). Several descriptive statistics, commonly used in dendrochronology, were calculated for standard chronologies prior the persistence was removed. These included standard deviation (SD), mean sensitivity (MS) and first-order autocorrelation (AC1).

3.3. Climate data

Monthly maximum, mean and minimum temperatures and precipitation data were obtained from three climate stations nearby our sample sites from the National Meteorological Information Centre (NMIC) of China (Fig. 1). Homogeneity was tested by applying the double-mass analysis, a graphical technique (Kohler, 1949). The monthly records from Deqin (28.48 °N, 98.92 °E, 3320 m a.s.l.) station contain heterogeneities, which are caused by the relocation of the station in January 1981 and April 1994. Therefore, Deqin station data were excluded from further analysis, despite its close location to the HP site. A regional meteorological data series was developed from

Table 2
Statistics of calibration and leave one-out verification results for the common period 1958–2004. R, correlation coefficient; SE, standard error of the estimate; ST, sign test, which counts the number of agreements and disagreements between the reconstructed and the instrumental climatic data; Pmt, product mean test; RE, reduction of error. Any positive value of RE indicates that there is confidence in the reconstruction (Fritts, 1976)

Calibration (model: $Y=6.076+4.419X$)								
Period	R		R^2		RR^2_{adj}		SE	
1958–2004	0.64		0.409		0.396		0.35	
Standard verification	1st difference verification							
Period	R	ST	Pmt	RE	R	ST	Pmt	RE
1958–2004	0.60**	33/14**	3.31**	0.36	0.80**	35/11**	4.78**	0.63

**Significant at $p<0.01$.

monthly records of two nearby high elevation stations Shangri-la (27.83 °N, 98.76 °E, 3276 m a.s.l.) and Daocheng (29.05 °N, 100.3 °E, 3729 m a.s.l.) (Fig. 1), by applying the techniques outlined by Jones and Hulme (1996). The climate stations are located in approximately the same altitude than the tree-ring sites (Table 1).

The climate–tree growth relationships were investigated by using correlation analyses between tree-ring data and meteorological records for their common period 1958–2004. Prior to correlation analyses, the climate series were modelled and prewhitened by applying the autoregressive model (AR), with the AR order objectively determined by the minimum Akaike information criteria (ACI) procedure (Meko, 1981; Cook et al., 1999). Simple correlations were calculated between the tree-ring residual chronologies and prewhitened regional monthly climate variables (precipitation, mean temperature as well as maximum and minimum temperature) from July prior to growth to October of the current growth year. In addition, various seasonal means of climate variables and their correlations with tree-ring data were calculated.

4. Results

4.1. Regional climate variability

The analyses of climate data revealed that during the past fifty years regional mean temperatures (TEM) have been increasing significantly by 0.028 °C yr^{-1} and 0.033 °C yr^{-1} for summer and winter season, respectively (Fig. 3). However, this warming trend was mainly contributed by an increase of minimum temperatures (T_{min}) instead of maximum temperatures (T_{max}). The regional diurnal temperature ranges (DTR) have been decreasing since the early 1980s. Other meteorological observations from north China (Gou et al., 2008; and references therein), west Canada (Wilson and Luckman, 2003) and global (Easterling et al., 1997) indicate that during the twentieth century minimum temperatures were rising much more rapidly than maximum temperatures. However, the dramatic change in these temperature relationships in the central Hengduan Mountains occurred in the early 1980s (Fig. 3). The decrease of DTR can be attributed to an increased cloud cover: daytime T_{max} is reduced due to greater reflection of incoming radiation from the upper surface of clouds and night time T_{min} increases because of enhanced downward radiation from clouds (Dai et al., 1999).

4.2. Chronology statistics

The two spruce TRW chronologies ranged in length from 318 years at HP to 385 years at BTH site. Based on the EPS statistics, the TRW chronologies met signal strength acceptances after A.D. 1780 for HP and A.D. 1690 for BTH (Table 1; Fig. 4). The MXD chronologies met the 0.85 EPS criterion for signal strength acceptance after A.D. 1820 (HP) and A.D. 1750 (BTH), respectively (Fig. 5). The chronologies generally showed a low mean sensitivity (MS) and high first-order autocorrelation (AC1), which is typical for spruce trees in humid environments. Compared with the TRW chronologies, the MXD chronologies of *P. brachytyla* usually displayed lower MS, standard deviations (SD) and AC1 (Table 1). The mean inter-series correlations (Rbar) ranged from 0.41 to 0.59, which indicated that the developed chronologies contain considerable common signals, and were thus suitable for climate change studies.

Although the distance between these two sites was relatively far (~120 km), significant correlations were found between the paired two site chronologies. TRW chronologies and their 15-year low-pass filter components correlated with $r=0.39$ and $r=0.41$ respectively over 1780–2005 period (Fig. 4). The respective correlations between the two MXD chronologies (1820–2005) were 0.44 and 0.61 (Fig. 5). This suggested that spruce trees growing near the upper tree line are influenced by some common regional climate signal. In order to dampen possible site-specific effects on tree growth and to emphasize regional-scale climate signals, all tree-ring index series of TRW and MXD were averaged to form two regional chronologies (RC). The EPS statistics were above the threshold of 0.85 after A.D. 1690 for TRW and A.D. 1750 for MXD regional chronologies (Table 1).

4.3. Growth–climate relationships

Temperatures were generally the main factors influencing TRW and MXD for trees growing at humid high-elevation sites (Figs. 6, 7). The growth–climate responses were very similar for the two site chronologies and generally the regional chronologies show higher correlations with temperature than the individual site chronologies. For TRW, the positive influence of temperature was predominant, while the importance of precipitation was weak except for the positive impact of precipitation in January and August of the growth year (Fig. 6). For regional TRW residual chronology, temperatures during the winter season (prior November until current February) played a crucial role ($r=0.43$; $p<0.01$). Although the influence of temperature

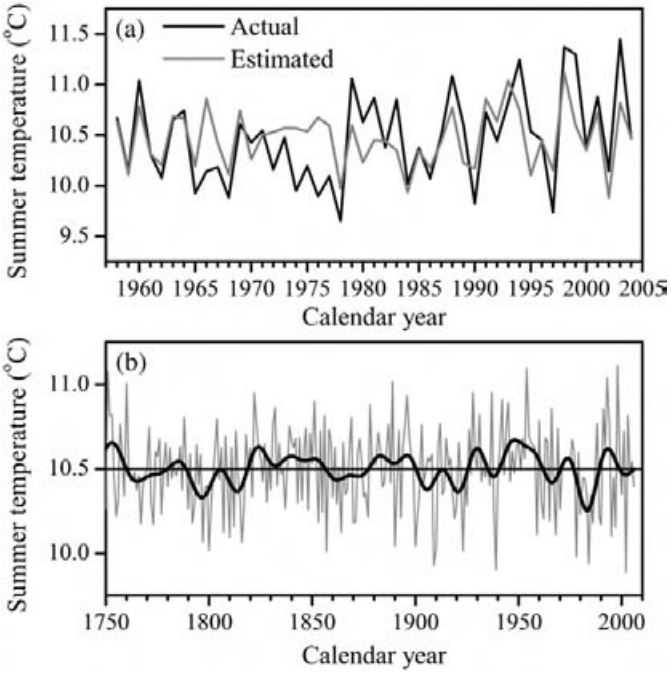

Fig. 8. (a) Comparison between actual and estimated mean warm season (April to September) temperature for their common period 1958–2004; (b) warm season temperature reconstruction for the central Hengduan Mountains derived from maximum latewood density. Thin line represents annual values; the bold line was smoothed with a 15-year low pass filter.

in the later growing season was also important, significant correlations only occurred for the current August.

MXD correlated with the temperature variations in the warm season of the current growth year (Fig. 7). Correlations between MXD residual chronologies and monthly mean temperature were significant from April to September except for June. The correlation between regional MXD residual chronology and warm season (April until September) mean temperature reached 0.64 ($p<0.01$), whereas split-summer temperature (April through September, excluding June) produced higher correlations ($r=0.72$, $p<0.01$) with regional MXD residual chronology. The summer daily maximum temperature (T_{max}) showed a stronger influence on MXD than the night-time minimum values (T_{min}). Precipitation in the growing season has mostly negative influence on MXD although positive correlations occur in August. Since the common signals between different TRW site chronologies were low (Fig. 4), more ring-width series are needed to develop a robust winter temperature reconstruction. Therefore, this paper concentrated on the warm season temperature reconstruction using the MXD chronologies.

4.4. Warm season temperature reconstruction

Based on the results of the growth–climate analyses, a transfer function was calculated based on a linear regression model, using the prewhitened mean summer temperature as the dependent variable and the regional MXD residual chronology as the independent variable. In order to reflect temperature variability for the whole warm season, April to September mean temperature was reconstructed for the study area. The reconstruction accounted for 40.9% of the actual summer temperature variances (Table 2), and agrees well with variations of the actual temperature during their common period 1958–2004 (Fig. 8a). The reconstructed summer temperature series covered the period A.D. 1750–2006 of reliable internal signal strength (Fig. 8b), based on the sample depths (>20 cores) and commonly acceptable EPS statistics (>0.85; Wigley et al., 1984) of the regional MXD chronology (Table 1).

The leave-one-out cross-validation method was employed to verify our reconstruction, since the meteorological data set available was too short to carry out a robust split-sample calibration (Michaelsen, 1987). Evaluative statistics include the Pearson's correlation coefficient (R), reduction of error (RE), product mean test (Pmt) and sign test (ST) (Fritts, 1976). The cross-validation test yielded a positive RE (0.36), indicating predictive skill of the regression model (Table 2). Statistically significant sign test and product mean test between the recorded data and the leave-one-out-derived estimates were additional indications for the reconstruction's validity. When 1st difference of the actual and leave-one-out estimated series were used, even better verification statistics were obtained, indicating that the developed model was successful in tracking the high-frequency temperature variability over the calibration period.

To demonstrate that our reconstruction and instrumental records reflected regional-scale temperature variability, we correlated these data with the CRUts 2.1 dataset (Mitchell and Jones, 2005) of all grid cells available for a user-defined region. The analyses were achieved using the KNMI climate explorer (Royal Netherlands Meteorological Institute; http://climexp.knmi.nl). Instrumentally recorded warm season temperatures in our study area (two stations means), as well as reconstructed summer temperatures, correlated significantly with gridded surface temperatures on a regional scale (Fig. 9). Spatial correlation fields were similar for the instrumental and reconstructed temperature variability, although correlations were lower for the latter. The highest correlation fields were confined to the north–south orientated Hengduan Mountain ranges. These results indicated that our summer temperature reconstruction represents climatic variations for a large territory in the Hengduan Mountains.

5. Discussion

5.1. Growth–climate response

Spruce ring-width chronologies from the upper timberline are sensitive to temperature, especially in the winter season (Fig. 6). This was also reported for other high elevation conifers from west Sichuan (Shao and Fan, 1999) and the eastern Tibetan Plateau (Bräuning, 2001; Gou et al., 2007; Liang et al., 2008). Winter temperatures have been found to constrain radial growth in different temperate species and ecosystems in eastern North American (Pederson et al., 2004). Warm conditions in the late autumn might increase carbohydrate storages in the stem, and thus enhance earlywood growth in the following spring (Gou et al., 2008). Cold late-winter conditions, on the other hand,

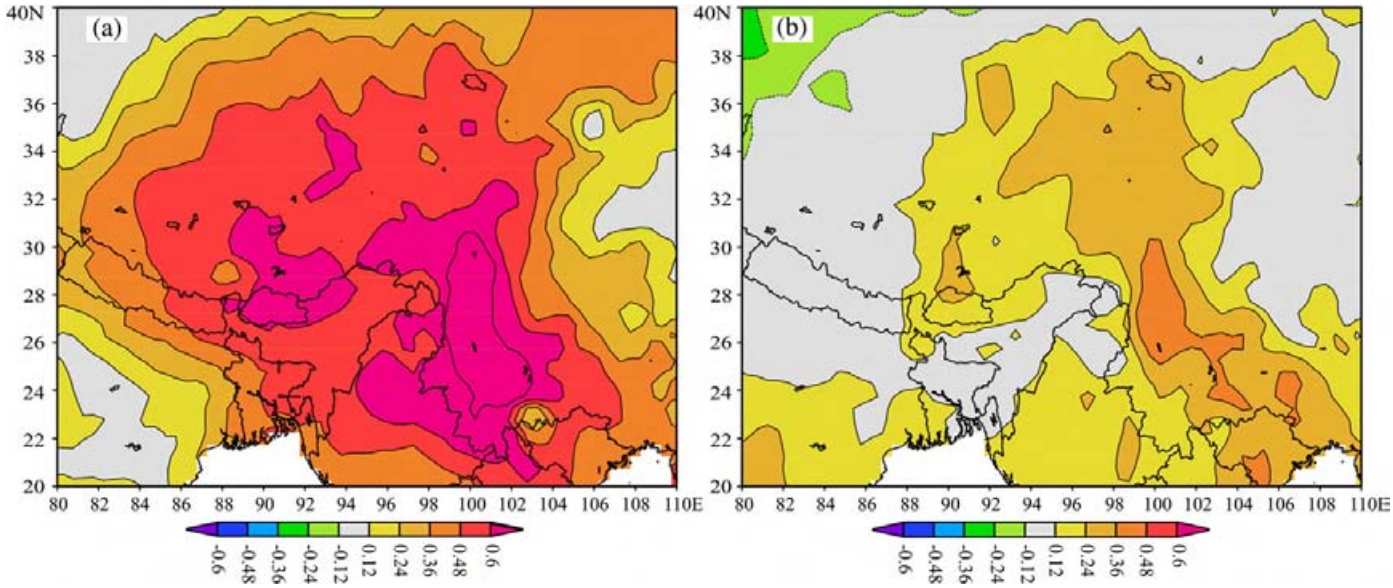

Fig. 9. Spatial correlations of (a) instrumental and (b) reconstructed summer (April–September) temperatures with regional gridded April–September temperatures for the period 1958–2001. The analyses were performed using the KNMI climate explorer (Royal Netherlands Meteorological; http://climexp.knmi.nl), the gridded climate dataset was developed by the Climatic Research Unit (Mitchell and Jones, 2005; CRUts 2.1).

might cause bud damage, frost desiccation, and fine root mortality due to low soil temperature (Körner, 1998). The growth–climate responses indicate that low night-time temperatures in the late winter probably cause frost damages and thus have a negative impact on radial growth (Fig. 6). High warm season temperatures stimulate ring-width growth, but significant correlations only occur with August.

Compared with TRW data, the MXD chronologies show a consistent response to a wider window of warm season temperature (Fig. 7). Similar results were reported by various studies and thus MXD was used for reconstructing summer temperature variations in the boreal and temperate climate zones (D'Arrigo et al., 1992; Schweingruber et al., 1993; Davi et al., 2003) and in subtropical mountain regions (Hughes, 2001; Davi et al., 2002; Bräuning and Mantwill, 2004). Temperature conditions influence the number and size of latewood cells, and needle mass which determines the amount of photosynthates available for cell wall thickening during the late growing season (Hughes, 2001; Vaganov et al., 2006). Warmer temperature during late summer can contribute to latewood cell wall thickening, thus produce denser latewood. Meanwhile, latewood formation appears to benefit from photosynthate production and elevated hormone levels in the early growth season (April–May) (Conkey, 1986; Vaganov et al., 2006). TRW at individual sites correlated with MXD chronologies over 1820–2005 period (r=0.12 for HP, 0.50 for BTH and 0.38 for RC, respectively), which indicates that particular years with narrow rings show corresponding lower values of latewood density. Annual rings formed under unfavourable environmental conditions consist of only several tracheids in a radial dimension with radial sizes smaller than usual and with thinner cell walls.

5.2. Comparison with regional records

Our warm season temperature reconstruction, as derived from MXD, contains inter-annual to multi-decadal temperature variability. Remarkable periods of high summer temperature occurred during 1750s, 1820–1850s, 1880–1890s, 1930–1950s and 1990–present. On the opposite, the periods 1790–1810s, 1860–1870s, 1900–1920s and 1960–1985 were relatively cold (Fig. 8). The spatial correlation analysis shows that our reconstruction captures a great part of the regional temperature variability of the Hengduan Mountains and the southeastern Tibetan Plateau (Fig. 9).

Several tree-ring based temperature reconstructions in surrounding areas have recently been developed (Shao and Fan, 1999; Bräuning and Mantwill, 2004; Liang et al., 2008). Based on MXD data of multispecies from 22 temperature sensitive sites, four growth regions were outlined from northeast to southwest of the Tibetan Plateau (Bräuning and Mantwill, 2004). Late summer (August–September) temperature reconstructions from the eastern (ETP) and southern (STP) region of Tibet (Figs. 1, 10) of those four growth regions are compared with our reconstruction. Shao and Fan (1999) developed four Balfour spruce (*Picea likiangensis* var. *balfouriana*) TRW chronologies and reconstructed winter (prior December to February) minimum temperature in west Sichuan (WS in Figs. 1, 10). Their calibration model explained 58% of the actual temperature variances for 1960–1993. Using four TRW series of Balfour spruce, Liang et al. (2008) developed a summer (June–August) minimum temperature reconstruction (R^2=0.27 for 1957–2002) for the upper source region of the Yangtze River on the Tibetan Plateau (SRY in Figs. 1, 10).

Our reconstruction mirrors similar warm/cold intervals as temperature reconstructions in the nearby regions (Fig. 10). Cold summers of 1810s, 1860s, 1900–1910s, and 1970s found in the present study are consistent with low summer temperatures in southern Tibet (Bräuning and Mantwill, 2004) and the source region of Yangtze river (Liang et al., 2008). Cold condition in the 1800s, 1900s and 1970s are also reported for the northeastern Tibetan Plateau (Gou et al., 2008), the Eastern Himalayan Region (Bhattacharyya and Chaudhary, 2003)

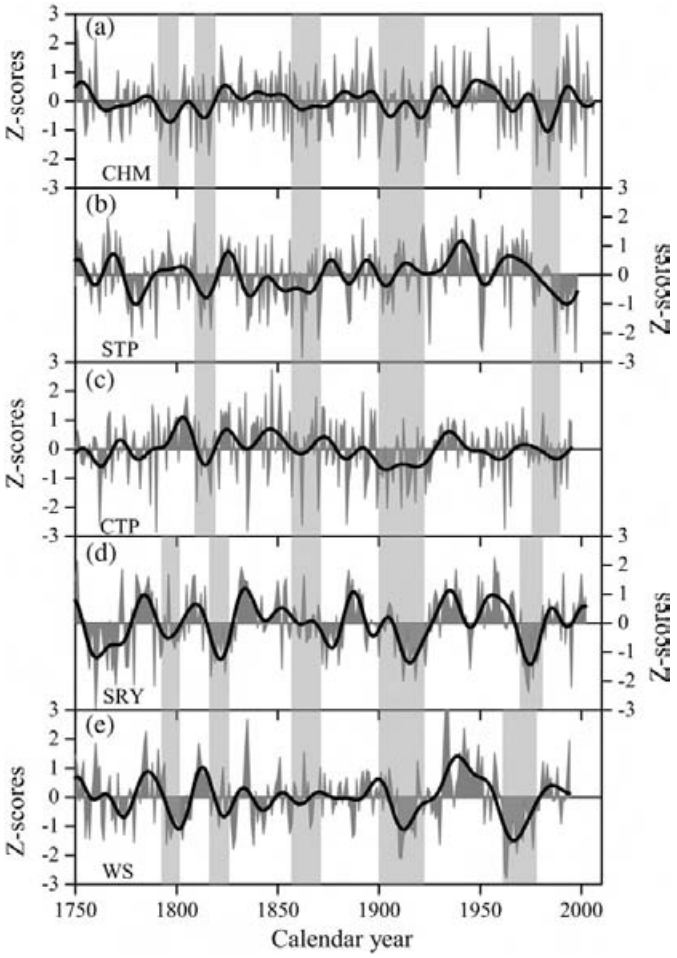

Fig. 10. Graphical comparison of various temperature reconstructions for the western China derived from tree-ring records. (a) warm season (April–September) mean temperature reconstruction in the central Hengduan Mountains (CHM; this study); (b) late-summer (August–September) reconstruction in the southern Tibetan Plateau (STP; Bräuning and Mantwill, 2004); (c) late-summer temperature reconstruction in the eastern Tibetan Plateau (ETP; Bräuning and Mantwill, 2004); (d) summer (June to August) minimum temperature reconstruction in the upper source region of Yangtze River (SYR; Liang et al., 2008); (e) winter half year temperature reconstruction from west Sichuan Plateau (WS; Shao and Fan, 1999). All series were adjusted for their long-term means over period 1750–1994, and smoothed with a 15-year low-pass filter to emphasize long-term fluctuations.

and Nepal (Cook et al., 2003). The warm 1820–1850s, 1880s, 1930–1950s are consistent between the compared records (Fig. 10), and were also reported as warm periods by Wu et al. (1988) in the Hengduan Mountain region, and in Kashmir (Western Himalaya; Hughes, 2001). Some differences existing between the reconstructions (i.e. in the 1760s, 1800s) may reflect the local influence of different geographic features or difference in seasonality of the various temperature reconstructions.

Advance and retreat phases of monsoonal-temperate glaciers are largely controlled by changes in temperature, especially by summer temperature (Shi, 2002; Yang et al., 2008). The cold periods of the 1800–1810s and 1900–1920s are consistent with glacier advances or standstill recorded from Lhamcoka (31°49′N, 99°06′E, 6168 m a.s.l.) in the Chola Shan (Bräuning, 2006). The warm 1930–1950s and the last two decades, as well as the cold 1960–1970s, are consistent with fluctuations of the nearby Mingyong glacier (28°29′N, 98°47′E, 6740 m a.s.l.) in the Meili Snow Mountain (Zheng et al., 1999; Baker and Moseley, 2007) and the Baishui No. 1 glacier (27°10′N, 100°13′E, 5600 m a.s.l.) of the Jade Dragon Snow Mountain (He et al., 2003).

The 1930–50s is likely the warmest period in the last few centuries seen in the tree-ring records, and was notable throughout the 20th century over China, especially in the south-western part of China and on the Tibetan Plateau (Wang et al., 2004). The cold period in the early 20th century and high temperatures in the 1940s and 1950s are also indicated by $\delta^{18}O$ variations in the Puruogangri and Malan ice cores in northern Tibet (Wang et al., 2003; Yao et al., 2006). The cooling in the 1960s and warming in the 1980s seems to be more pronounced and started earlier in the reconstructions of Shao and Fan (1999) and Liang et al. (2008). This may reflect asymmetric variation patterns of maximum and minimum temperatures during regional warming processes (Fig. 3). A delayed warming of summer maximum temperature after the 1980s in comparison with rising winter minimum temperature was observed in tree-ring based temperature reconstructions and meteorological records on the north-eastern Tibetan Plateau (Gou et al., 2008). It should be noted that MXD seems to be more strongly influenced by summer day-time maximum temperatures than by nighttime minimum values (Fig. 7; Wilson and Luckman, 2003); whereas there are considerable winter minimum temperature signals in ring-width chronologies of Liang et al. (2008), although their reconstruction concentrated on summer season temperatures.

6. Conclusions

We developed TRW and MXD series from two sites of *P. brachytyla* in the central Hengduan Mountains, where previously high-resolution climate proxies were missing. TRW and MXD series are most sensitive to regional temperatures variation, whereas MXD shows a strong response to temperature variability in the summer season. Based on MXD data, a warm season (April to September) mean temperature was reconstructed over the past 257 years. Spatial correlation fields using instrumental and reconstructed series reveal similar patterns, indicating that our reconstruction represents a high degree of regional summer temperature variability over the Hengduan Mountains. Comparison with other tree ring-based temperature reconstructions shows high coherency in the timing of warm/cold episodes at the decadal scale across the Tibetan Plateau, i.e. cold 1800s, 1860s, 1900–1910s, 1970s; and warm 1750s, 1825–1850s, 1880s, 1930–50s. The spatiotemporal discrepancies among different temperature reconstructions may reflect the influences of different geographic features; bands of climatic signals preserved, and target season windows. Therefore, further efforts should be taken to develop more comprehensive tree-ring networks, and to combine various tree-ring parameters like maximum latewood density and stable isotopes, to shed more light on the spatial and temporal variability of the past climate changes in this environmentally sensitive region.

Acknowledgements

The authors thank Mrs. Iris Burchardt for her aid on tree-ring measurements. We also thank Dr. Liang E.Y. and Prof. Shao X.M. who kindly provided their data. Particular thanks are extended to two anonymous reviewers for their valuable suggestions and comments regarding revision of the manuscript. Spatial field correlations were generated using the KNMI Climate Explorer (http://climexp.knmi.nl). This work was financially supported by the National Science Foundation of China (No. 90302013) and the Max-Planck-Gesellschaft. Bao Yang was supported by the 100 talents project of the Chinese Academy of Sciences (29082762).

References

Baker, B.B., Moseley, R.K., 2007. Advancing treeline and retreating glaciers: implications for conservation in Yunnan, P.R. China. Arct. Antarct. Alp. Res. 39 (2), 200–209.
Bhattacharyya, A., Chaudhary, V., 2003. Late-summer temperature reconstruction of the eastern Himalayan region based on tree-ring data of *Abies densa*. Arct. Antarct. Alp. Res. 35 (2), 196–202.
Bräuning, A., 1994. Dendrochronology for the last 1400 years in eastern Tibet. GeoJ. 34, 75–95.
Bräuning, A., 2001. Combined view of various tree ring parameters from different forest habitats in Tibet for the reconstruction of seasonal aspects of Asian monsoon variability. Palaeobotanist 50, 1–12.
Bräuning, A., 2006. Tree-ring evidence of 'Little Ice Age' glacier advances in southern Tibet. Holocene 16 (3), 369–380.
Bräuning, A., Mantwill, B., 2004. Summer temperature and summer monsoon history on the Tibetan Plateau during the last 400 years recorded by tree rings. Geophys. Res. Lett. 31, L24205. doi:10.1029/2004GL020793.
Bräuning, A., Grießinger, J., 2006. Late Holocene variations in monsoon intensity in the Tibetan–Himalayan region-evidence from tree rings. J. Geol. Soc. India 68 (3), 485–494.
Briffa, K., Jones, P.D., Schweingruber, F.H., 1988. Summer temperature patterns over Europe: a reconstruction from 1750 A.D. based on maximum latewood density indices of conifers. Quat. Res. 30, 36–52.
Briffa, K.R., Osborn, T.J., Schweingruber, F.H., Harris, I.C., Jones, P.D., Shiyatov, S.G., Vaganov, E.A., 2001. Low frequency temperature variations from a northern tree ring density network. J. Geophys. Res. 106, 2929–2941.
Briffa, K.R., Osborn, T.J., Schweingruber, F.H., 2004. Large-scale temperature inferences from tree rings: a review. Glob. Planet. Change 40, 11–26.
Büntgen, U., Frank, D.C., Nievergelt, D., Esper, J., 2006. Summer temperature variations in the European Alps, A.D. 755–2004. J. Climate 19 (21), 5606–5623.
Büntgen, U., Frank, D.C., Grudd, H., Esper, J., 2008. Long-term summer temperature variations in the Pyrenees. Clim. Dyn. 31 (6), 615–631.
Chang, D.H.S., 1981. The vegetation zonation of the Tibetan Plateau. Mt. Res. Dev. 1 (1), 29–48.
Conkey, L.E., 1986. Red spruce tree-ring widths and densities in eastern North America as indicators of past climate. Quat. Res. 26, 232–243.
Cook, E.R., 1985. A time-series analysis approach to tree-ring standardization. Ph.D. Thesis, Arizona Uni. Press, Tucson.
Cook, E.R., Kairiukstis, L.A., 1990. Methods of Dendrochronology. Kluwer Academic Press, Netherlands.
Cook, E.R., Peters, K., 1997. Calculating unbiased tree-ring indices for the study of climatic and environmental change. Holocene 7, 361–370.
Cook, E.R., Meko, D.M., Stahle, D.W., Cleaveland, M.K., 1999. Drought reconstructions for the continental United States. J. Climate 12, 1145–1162.
Cook, E.R., Krusic, P.J., Jones, P.D., 2003. Dendroclimatic signals in long tree-ring chronologies from the Himalayas of Nepal. Int. J. Climatol. 23, 707–732.
D Arrigo , R.D., Jacoby, G.C., Free, R.M., 1992. Tree-ring width and maximum latewood density at the North American tree line: parameters of climatic change. Can. J. For. Res. 22, 1290–1296.
D Arrigo , R.D., Mashig, E., Frank, D.C., Jacoby, G.C., Wilson, R., 2004. Reconstructed warm season temperature for Nome, Seward, Peninsula, Alaska. Geophys. Res. Lett. 31, L09202. doi:10.1029/2004GL019756.
Dai, A., Trenberth, K.E., Karl, R., 1999. Effects of clouds, soil moisture, precipitation, and water vapour on diurnal temperature range. J. Climate 12 (8), 2451–2473.
Davi, N.K., D'Arrigo , R.D., Jacoby, G.C., Buckley, B., Kobayashi, O., 2002. Warm-season annual to decadal temperature variability for Hokkaido, Japan, inferred from maximum latewood density (AD 1557–1990) and ring width data (AD 1523–1990). Clim. Change 52, 201–217.
Davi, N.K., Jacoby, G.C., Wiles, G.C., 2003. Boreal temperature variability inferred from maximum latewood density and tree-ring width data, Wrangell Mountain region, Alaska. Quat. Res. 60, 252–262.
Easterling, D.R., Horton, B., Jones, P.D., Peterson, T.C., Karl, T.R., Parker, D.E., Salinger, M.J., Razuvayev, V., Plummer, N., Jamerson, P., Folland, C., 1997. Maximum and minimum temperature trends for the global. Science 277, 364–367.
Frank, D., Esper, J., 2005. Temperature reconstructions and comparisons with instrumental data from a tree-ring network for the European Alps. Int. J. Climatol. 25 (11), 1437–1454.
Fritts, H.C., 1976. Tree-Rings and Climate. Academic Press, London.
Gou, X., Chen, F., Jacoby, G., Cook, E.R., Yang, M., Peng, J., Zhang, Y., 2007. Rapid tree growth with respect to the last 400 years in response to climate warming, northeastern Tibetan Plateau. Int. J. Climatol. 27, 1497–1503.
Gou, X.H., Chen, F.H., Yang, M.X., Gordon, J., Fang, K.Y., Tian, Q.H., Zhang, Y., 2008. Asymmetric variability between maximum and minimum temperatures in Northeastern Tibetan Plateau: evidence from tree rings. Sci. China Ser. D 51 (1), 41–55.
He, Y.Q., Zhang, Z.L., Yao, T.D., Chen, T., Pang, H.X., Zhang, D., 2003. Modern changes of the climate and glaciers in China's monsoonal temperature glacier region. Acta Geogr. Sin. 58 (4), 550–558 (in Chinese, with English Abstr.).
Hughes, M.K., 2001. An improved reconstruction of summer temperature at Srinagar, Kashmir since 1660 AD, based on tree-ring width and maximum latewood density of *Abies pindrow* [Royle] Spach. Palaeobotanist 50, 13–19.
Jones, P.D., Hulme, M., 1996. Calculating regional climatic time series of temperature and precipitation: methods and illustrations. Int. J. Climatol. 16, 361–377.
Kang, X.C., Graumlich, L.J., Sheppard, P.R., 1997. A 1835-year tree-ring chronology and its preliminary analysis in Dulan region, Qinghai. Chin. Sci. Bull. 42 (13), 1122–1124.
Kirdyanov, A.V., Treydte, K.S., Nikolaev, A., Helle, G., Schleser, G.H., 2008. Climate signals in tree-ring width, density and $\delta^{13}C$ from larches in Eastern Siberia (Russia). Chem. Geol. 252, 31–41.
Kohler, M.A., 1949. On the use of double-mass analysis for testing the consistency of meteorological records and for making required adjustments. Bull. Am. Meteorol. Soc. 30 (5), 188–189.
Körner, C., 1998. A re-assessment of high elevation treeline positions and their explanation. Oecologia 115, 445–459.
Liang, E., Shao, X., Qin, N., 2008. Tree-ring based summer temperature reconstruction for the source region of the Yangtze River on the Tibetan Plateau. Glob. Planet. Change 61, 313–320.

Liu, X.H., Qin, D.H., Shao, X.M., Chen, T., Ren, J.W., 2005. Temperature variations recovered from tree-rings in the middle Qilian Mountain over the last millennium. Sci. China Ser. D 48, 521–529.
Luckman, B.H., Wilson, R.J.S., 2005. Summer temperature in the Canadian Rockies during the last millennium: a revised record. Clim. Dyn. 24, 131–144.
Meko, D.M., 1981. Applications of Box–Jenkins methods of time series analysis to the reconstruction of drought from tree rings. Ph.D. Thesis, Univ. Arizona, Tucson.
Michaelsen, J., 1987. Cross-validation in statistical climate forecast models. J. Appl. Meteorol. Clim. 26, 1589–1600.
Mitchell, T.D., Jones, P.D., 2005. An improved method of constructing a database of monthly climate observations and associated high-resolution grids. Int. J. Climatol. 25, 639–712.
Osborn, T.J., Briffa, K.R., Jones, P.D., 1997. Adjusting variance for sample size in tree-ring chronologies and other regional mean timeseries. Dendrochronologia 15, 89–99.
Pederson, N., Cool, E.R., Jacoby, G.C., Peteet, D.M., Griffin, K.L., 2004. The influence of winter temperatures on the annual radial growth of six northern range margin tree species. Dendrochronologia 22, 7–29.
Rinn, F., 1996. TSAPWin: time series analysis and presentation for dendrochronology and related applications. Version 0.55 User reference. Heidelberg, p. 76.
Schinker, M.G., Hansen, N., Spiecker, H., 2003. High-frequency densitometry — a new method for the rapid evaluation of wood density variations. IAWA J. 24 (3), 231–239.
Schweingruber, F.H., Briffa, K.R., 1996. Tree-ring density networks of climate reconstruction. In: Jones, P.D., Bradley, R.S., Jouzel, J. (Eds.), Climatic Variations and Forcing Mechanisms of the Last 2000 Years. . NATO ASI Series, vol. 41. Springer-Verlag, Berlin, pp. 43–66.
Schweingruber, F.H., Briffa, K.R., Nogler, P., 1993. A tree-ring densitometric transect from Alaska to Labrador: comparison of ring-width and maximum-latewood-density chronologies in the conifer belt of northern North America. Int. J. Biometeorol. 37, 151–169.
Shao, X.M., Fan, J.M., 1999. Past climate on west Sichuan Plateau as reconstructed from ring-widths of dragon spruce. Quat. Sci. 1, 81–89 (in Chinese, with English Abstr.).
Shi, Y.F., 2002. Characteristics of late Quaternary monsoonal glaciation on the Tibetan Plateau and in East Asia. Quat. Int. 97–98, 79–81.
Stokes, M.A., Smiley, T.L., 1996. An Introduction to Tree-ring Dating. Arizona Uni. Press, Chicago, p. 73. London.
Vaganov, E.A., Hughes, M.K., Shashkin, A.V., 2006. Growth dynamics of conifer tree rings-images of past and future environments. Ecological Studies, vol. 183. Springer-Verlag, Berlin, Heidelberg.
Wang, L.L., Payette, S., Bégin, Y., 2001. 1300-year tree-ring width and density series based on living, dead and subfossil black spruce at tree-line in Subarctic Québec, Canada. Holocene 11 (3), 333–341.
Wang, N.L., Yao, T.D., Pu, J.C., Zhang, Y.L., Sun, W.Z., Wang, Y.Q., 2003. Variations in air temperature during the last 100 years revealed by $\delta^{18}O$ in the Malan ice core from the Tibetan Plateau. Chin. Sci. Bull. 48, 2134–2138.
Wang, S.W., Zhu, J.H., Cai, J.N., 2004. Interdecadal variability of temperature and precipitation in China since 1880. Adv. Atmos. Sci. 21 (3), 307–313.
Webster, P.J., Magaña, V.O., Palmer, T.N., Shukla, J., Tomas, P.A., Yanai, M., Yasunari, T., 1998. Monsoons: processes, predictability, and the prospects for prediction. J. Geophys. Res. 103 (C7), 14451–14510.
Wigley, T., Briffa, K.R., Jones, P.D., 1984. On the average value of correlated time series, with applications in dendroclimatology and hydrometeorology. J. Clim. Appl. Meteorol. 23, 201–213.
Wilson, R.J.S., Luckman, B.H., 2003. Dendroclimatic reconstruction of maximum summer temperatures from upper treeline sites in Interior British Columbia, Canada. Holocene 13 (6), 851–861.
Wu, X.D., Lin, Z.Y., Sun, L., 1988. A preliminary study on the climatic change of the Hengduan Mountains area since 1600 A.D. Adv. Atmos. Sci. 5 (4), 437–443.
Wu, X.D., Sun, L., Zhan, X.Z., 1989. A preliminary study on reconstructing past climate in the middle Xizang Plateau by using tree-ring data. Acta Geogr. Sin. 44 (3), 334–342 (in Chinese, with English Abstr.).
Xu, X.D., Miao, Q.J., Wang, J., Zhang, X.J., 2003. The water vapour transport model at the regional boundary during the Meiyu Period. Adv. Atmos. Sci. 20, 333–342.
Yang, B., Bräuning, A., Dong, Z., Zhang, Z., Jiao, K., 2008. Late Holocene monsoonal temperature glacier fluctuations on the Tibetan Plateau. Glob. Planet. Change 60, 126–140.
Yao, T.D., Guo, X.J., Thompson, L., Duan, K.Q., Wang, N.L., Pu, J.C., Xu, B.Q., Yang, X.X., Sun, W.Z., 2006. $\delta^{18}O$ record and temperature change over the past 100 years in ice cores on the Tibetan Plateau. Sci. China Ser. D 49, 1–9.
Zheng, B.X., Zhao, X.T., Li, T.S., Wang, C.Y., 1999. Features and fluctuation of the Melang glacier in the Mainri Mountain. J. Glaciol. Geocryology 21 (2), 145–150 (in Chinese, with English Abstr.).